Developmental Biology 435 (2018) 6–14

Contents lists available at ScienceDirect

Developmental Biology

journal homepage: www.elsevier.com/locate/developmentalbiology

Luteinizing hormone signaling phosphorylates and activates the cyclic GMP phosphodiesterase PDE5 in mouse ovarian follicles, contributing an additional component to the hormonally induced decrease in cyclic GMP that reinitiates meiosis

Jeremy R. Egbert[a,*], Siu-Pok Yee[a,b], Laurinda A. Jaffe[a]

[a] Department of Cell Biology, UConn Health, 263 Farmington Ave, Farmington, CT 06030, USA
[b] Center for Mouse Genome Modification, UConn Health, 263 Farmington Ave, Farmington, CT 06030, USA

ARTICLE INFO

Keywords:
Ovarian follicle
Oocyte
Cyclic GMP
Phosphodiesterase
PDE5
Meiosis

ABSTRACT

Prior to birth, oocytes within mammalian ovarian follicles initiate meiosis, but then arrest in prophase until puberty, when with each reproductive cycle, one or more follicles are stimulated by luteinizing hormone (LH) to resume meiosis in preparation for fertilization. Within preovulatory follicles, granulosa cells produce high levels of cGMP, which diffuses into the oocyte to maintain meiotic arrest. LH signaling restarts meiosis by rapidly lowering the levels of cGMP in the follicle and oocyte. Part of this decrease is mediated by the dephosphorylation and inactivation the NPR2 guanylyl cyclase in response to LH, but the mechanism for the remainder of the cGMP decrease is unknown. At least one cGMP phosphodiesterase, PDE5, is activated by LH signaling, which would contribute to lowering cGMP. PDE5 exhibits increased cGMP-hydrolytic activity when phosphorylated on serine 92, and we recently demonstrated that LH signaling phosphorylates PDE5 on this serine and increases its activity in rat follicles. To test the extent to which this mechanism contributes to the cGMP decrease that restarts meiosis, we generated a mouse line in which serine 92 was mutated to alanine (*Pde5-S92A*), such that it cannot be phosphorylated. Here we show that PDE5 phosphorylation is required for the LH-induced increase in cGMP-hydrolytic activity, but that this increase has only a modest effect on the LH-induced cGMP decrease in mouse follicles, and does not affect the timing of meiotic resumption. Though we show that the activation of PDE5 is among the mechanisms contributing to the cGMP decrease, these results suggest that another cGMP phosphodiesterase is also activated by LH signaling.

1. Introduction

In mammals, the oocyte cell cycle arrests at the diplotene stage of meiotic prophase before birth, and remains arrested throughout all stages of growth. Beginning at puberty, cyclic secretion of follicle stimulating hormone (FSH) from the pituitary supports a cohort of follicles through the final stages of growth to reach the preovulatory stage. Then, during each reproductive cycle, a brief surge in circulating luteinizing hormone (LH) acts on one or more preovulatory follicles to initiate many different signaling cascades that result in a multitude of responses, including oocyte meiotic resumption (Jaffe and Egbert, 2017), activation of the GLYT1 transporter to regulate osmotic balance in the oocyte (Richard and Baltz, 2017), cumulus expansion and ovulation (Hunzicker-Dunn and Mayo, 2014), and formation of the corpus luteum (Stocco et al., 2007). These LH-dependent events occur on different time scales, but one of the most rapid is the activation of mechanisms that lead to the resumption of oocyte meiosis (Shuhaibar et al., 2015).

Within preovulatory follicles, oocyte meiotic arrest is maintained by high levels of cGMP, which is produced in the surrounding granulosa and cumulus cells and diffuses into the oocyte through gap junctions (Norris et al., 2009; Vaccari et al., 2009; Shuhaibar et al., 2015). Follicle cGMP is produced by the membrane guanylyl cyclase natriuretic peptide receptor 2 (NPR2; also called guanylyl cyclase-B or GC-B), which is required for meiotic arrest (Zhang et al., 2010). Follicles from mice lacking functional NPR2 contain no detectable cGMP (Geister et al., 2013), indicating that NPR2 activity accounts for most, if not all, of the cGMP produced in the follicle. Upon exposure to a surge of LH, cGMP levels rapidly decline in the outer granulosa cells, falling from ~ 4 to 0.1 μM by 20 min (Shuhaibar et al., 2015). This reverses the

* Corresponding author.
E-mail addresses: egbert@uchc.edu (J.R. Egbert), syee@uchc.edu (S.-P. Yee), ljaffe@uchc.edu (L.A. Jaffe).

https://doi.org/10.1016/j.ydbio.2018.01.008
Received 29 November 2017; Received in revised form 10 January 2018; Accepted 11 January 2018
Available online 16 January 2018
0012-1606/

concentration gradient such that cGMP diffuses out of the oocyte (Shuhaibar et al., 2015), thus allowing meiosis to proceed.

A major component of the cGMP decrease is the rapid inactivation of NPR2 (Robinson et al., 2012) by dephosphorylation in response to LH signaling (Egbert et al., 2014). NPR2 activity is regulated by the binding of its agonist C-type natriuretic peptide (CNP) and by phosphorylation on some combination of 7 juxtamembrane serines and threonines (Potter, 2011). If these 7 sites are mutated to glutamate (NPR2-7E), the enzyme behaves as though it is constitutively phosphorylated and cannot be inactivated by dephosphorylation (Yoder et al., 2012). We previously generated mice homozygous for a global knockin of a sequence in which the 7 regulatory phosphorylation sites of NPR2 are mutated to glutamate ($Npr2^{7E/7E}$) (Shuhaibar et al., 2016). In isolated preovulatory follicles from these $Npr2^{7E/7E}$ mice, the LH-induced cGMP decrease in the mural granulosa cells is significantly attenuated (Shuhaibar et al., 2016), reaching a plateau of ~ 0.3 μM cGMP (see Fig. 3E below), in contrast to the ~ 0.1 μM level observed in the wild type (Shuhaibar et al., 2015). This attenuation of the cGMP decrease is sufficient to delay meiotic resumption by ~ 5 h (Shuhaibar et al., 2016), but a substantial part of the LH-induced cGMP decrease remains unexplained. These findings suggest that LH signaling could increase the activity of one or more phosphodiesterases (PDEs), which would contribute to the follicle cGMP decrease.

In rat follicles, most of the basal cGMP-hydrolytic activity is explained by PDE1 and PDE5 (Egbert et al., 2016). PDE1 is activated by calcium (Bender and Beavo, 2006), and PDE5 activity is increased by PKA- or PKG-dependent phosphorylation of serine 92 (Corbin et al., 2002; Jäger et al., 2010). We have previously shown that LH signaling induces the phosphorylation of PDE5 on serine 92 in rat follicles, which is associated with an ~ 70% increase in cGMP-hydrolytic activity (Egbert et al., 2016). We also showed that the increase in PDE5 phosphorylation and activity in response to LH could be prevented by the PKA inhibitor H89 (Egbert et al., 2016). However, since PKA has many other substrates, and since H89 lacks complete specificity for PKA (Davies et al., 2000; Murray, 2008), it remained uncertain whether the phosphorylation of PDE5 was directly responsible for its activation. Furthermore, these experiments did not determine how much the activation of PDE5 contributes to the LH-induced cGMP decrease in follicles, which triggers oocyte meiotic resumption. In this study, we tested the hypotheses that 1) phosphorylation of PDE5 is required for the LH-induced increase in its hydrolytic activity, 2) the increase in PDE5 activity contributes to the follicle cGMP decrease, and 3) preventing the phosphorylation and activation of PDE5 delays meiotic resumption in response to LH. To do this, we generated a mouse line in which serine 92 of PDE5 was mutated to alanine (*Pde5-S92A*) in all tissues, such that it cannot be phosphorylated. We show that this mutation prevents the increase in PDE5 activity in response to LH. Furthermore, our data indicate that the phosphorylation and activation of PDE5 contributes an additional component to the LH-induced cGMP decrease. Although we confirm previous reports that total PDE5 activity plays a role in the timing of meiotic resumption, we find that preventing the *increase* in hydrolytic activity due to PDE5 phosphorylation does not affect the timing of meiotic resumption in response to LH. These data suggest that the activation of PDE5 by phosphorylation is a redundant mechanism for lowering cGMP levels in mouse ovarian follicles, and indicate that the activation of at least one other phosphodiesterase in response to LH signaling contributes to the cGMP decrease that restarts meiosis.

2. Materials and methods

2.1. Mice and follicle isolation/culture

The *Pde5-S92A* mouse line was generated by CRISPR/Cas9-mediated homology-directed repair to substitute alanine for serine 92, using C57BL/6J mice. Detailed information about the generation and genotyping of these mice can be found in the Supplementary text and Supplementary Fig. S1. Mice homozygous for the *Pde5-S92A* mutation were viable, fertile (see Supplementary Fig. S2), and showed no obvious signs of morphological or behavioral abnormalities compared with wild-type mice from this mouse line.

Generation of the *Npr2-7E* mouse line was described by Shuhaibar et al. (2016); mice expressing the cGi500 Förster resonance energy transfer (FRET) sensor for cGMP were provided by Robert Feil (Thunemann et al., 2013). Wild-type mice were obtained from the generation of the *Pde5-S92A* line except for some of the mice used for Fig. 1, which were B6SJLF1/J animals obtained from The Jackson Laboratory (Bar Harbor, ME). All experiments were performed according to National Institutes of Health guidelines, and were approved by the UConn Health Institutional Animal Care and Use Committee.

Ovaries were removed from mice aged 23–27 days, and preovulatory follicles (~ 300–400 μm diameter) were dissected with fine forceps in MEMα (Gibco 12000022, Thermo Fisher, Waltham, MA) supplemented with 25 mM $NaHCO_3$, 3 mg/ml BSA, 5 μg/ml insulin, 5 μg/ml transferrin, 5 ng/ml selenium, 50 μg/ml streptomycin, 75 μg/ml penicillin G, and purified ovine follicle stimulating hormone (FSH) (A.F. Parlow, National Hormone and Peptide Program; NHPP). Follicles were plated on Millicell culture dish inserts (PICMORG50, Millipore Sigma, Billerica, MA) and cultured overnight at 37 °C in 5% CO_2 in the presence of 30 ng/ml FSH (except for two experiments of each genotype in Fig. 2E, which used 10 ng/ml FSH). During this culture on the Millicell membranes, follicles flatten to ~ 200 μm thick, and the presence of a nuclear membrane/nucleolus can be visualized using a 20×/0.4 NA long-working distance objective (Norris et al., 2007). Follicles that were too dark to see the oocyte, or oocytes that had undergone spontaneous nuclear envelope breakdown (NEBD), were not used for experiments. Treatments were applied to the medium below the Millicell and mixed by tipping the membrane several times. Except for Fig. 4B and D, purified ovine LH (NHPP) was used at a saturating concentration of 10 μg/ml (~ 350 nM) in all experiments. For the experiments in Fig. 4B and D, 0.1 μg/ml LH was used because it was the lowest concentration to achieve maximal NEBD in mouse follicle-enclosed oocytes (Mehlmann et al., 2006). LH was applied 23–30 h after FSH was applied to follicles.

2.2. Phos-tag gel electrophoresis and western blot

Equal numbers of follicles (11–17 per experiment) were treated with either LH or control vehicle (PBS) for 30 min, and then lysed by probe sonication in 60 μl Laemmli sample buffer with 75 mM dithiothreitol, 10 mM sodium fluoride, 1 mM sodium orthovanadate, 1 mM Pefabloc (Roche Diagnostics, Indianapolis, IN), and 1× Complete Protease Inhibitor, EDTA-free (Roche Diagnostics). Lysates were stored at −80 °C until the entire 60 μl volume was run on a gel containing 25 μM Phos-tag-acrylamide (Wako Chemicals USA, Richmond, VA) as previously described (Egbert et al., 2014, 2016). Phos-tag retards the migration of phosphorylated proteins through the gel, thus separating them from their non-phosphorylated forms (Kinoshita et al., 2006). Ponceau S (Thermo Fisher) was used to confirm equal loading of lanes following transfer to a nitrocellulose membrane. The membrane was blocked with 5% nonfat dry milk and probed with a rabbit total PDE5 antibody (17379-5(1), custom ordered from ProSci, Inc., Poway, CA) as previously described (Egbert et al., 2016). An index of PDE5 phosphorylation was generated by quantifying the ratio of the intensity of the upper (phosphorylated) band region to the intensity of the lower (non-phosphorylated) band using ImageJ software, as previously described (Egbert et al., 2014, 2016). The intensities of these regions were measured by drawing a rectangle around the lower band and then positioning an identical rectangle just above it, which encompassed the upper band in samples treated with LH.

2.3. Standard SDS-PAGE and western blot for PDE5 and PDE6

Follicle lysates were prepared in Laemmli sample buffer as described above; approximately 20 μg of follicle protein was loaded based on previous measurements of 3.5 μg protein/follicle (Norris et al., 2008). Lysates from mouse retina and lung tissue were prepared by probe sonication in 1% SDS with 1 mM Pefabloc and 1× Complete Protease Inhibitor, EDTA-free. Protein concentration was determined by bicinchoninic acid (BCA) assay (Thermo Fisher), and lysates were diluted in Laemmli sample buffer with 75 mM DTT prior to loading 0.1 μg or 0.3 μg of retina, or 1 μg or 2 μg of lung. Samples were run on 4–15% TGX gradient gels (Bio-Rad, Carlsbad, CA) in standard SDS-PAGE buffer (15 mA/gel for 80 min), transferred to nitrocellulose membranes (100 V for 90 min), and blocked in either 2% or 5% nonfat dry milk in Tris-buffered saline with 0.1% Tween-20. The blots were probed with rabbit antibodies for total PDE6A and PDE6B (21200-1-AP and 22063-1-AP, respectively; Proteintech, Rosemont, IL), and total PDE5 (ProSci 17379-5(1)). They were detected with a goat-anti-rabbit secondary antibody conjugated to horseradish peroxidase (R-05072-500, Advansta, Menlo Park, CA) and WesternBright ECL substrate (Advansta), and imaged by CCD camera (G: BOX Chemi XT4, Syngene, Frederick, MD).

2.4. Measurement of PDE5 cGMP-hydrolytic activity

Follicles were treated with either LH or PBS for 30 min and then solubilized by probe sonication in PDE lysis buffer containing 2 mM EGTA as previously described (Egbert et al., 2016). BCA assay was used to quantify the lysate protein concentrations. Lysates were stored at −80 °C until use within 10 days after lysate preparation. PDE assays were performed as previously described (Egbert et al., 2016) using 13–20 μg follicle protein and 30 nM ^{3}H-cGMP (7.1×10^{6} μCi/mmol; Perkin-Elmer, Waltham, MA) as substrate. To determine PDE5 activity, we assayed each sample in the absence and presence of the PDE5/6 inhibitor sildenafil (30 or 100 nM; Tocris, Minneapolis, MN) and calculated the difference between these two activities, as previously described (Egbert et al., 2016; see Fig. 2D).

2.5. Live confocal imaging of relative follicle cGMP levels

Following overnight culture, follicles expressing one copy of the cGi500 FRET sensor for cGMP (EC_{50} = 500 nM) (Thunemann et al., 2013) were placed in the 200 μm-deep channel of a perfusion slide (ibidi, Martinsried, Germany) that was covered with a glass cover slip (ibidi) attached with a thin layer of silicone grease (Shuhaibar et al., 2015). The perfusion ports were filled with medium and follicles were imaged using a Zeiss Pascal confocal system with a 40×/1.2 NA C-Apochromat objective lens with Immersol (Carl Zeiss Microscopy, Jena, Germany) as previously described (Shuhaibar et al., 2015). Images focused on the oocyte equator were collected every 30 s. After recording a 5-min baseline (20 scans), the medium was aspirated from both slide ports and replaced with medium containing LH through a single port.

Cyan fluorescent protein (CFP) and yellow fluorescent protein (YFP) emission intensities were measured in the outer 25 μm of the mural granulosa region using ImageJ as previously described (Shuhaibar et al., 2015); values were corrected for background and spectral bleedthrough. Since cGMP binding to cGi500 leads to less FRET between CFP and YFP (Russwurm et al., 2007), the CFP/YFP intensity ratio was used as an indicator of relative cGMP concentration (Thunemann et al., 2013; Shuhaibar et al., 2015).

2.6. Estimation of follicle cGMP concentrations

To estimate cGMP concentrations from the cGi500 CFP/YFP ratios, we generated an approximate calibration using ELISA measurements of cGMP in mouse follicles before LH (~ 4 μM) and after LH (~ 0.1 μM) reported by Shuhaibar et al. (2015). Importantly, these concentrations are situated near the top and bottom of the curve that represents the relationship between the $\log_{10}$[cGMP] and the CFP/YFP ratio for cGi500 recombinant protein (Russwurm et al., 2007), thus allowing us to model a logistic curve. We applied these two concentrations (4 μM and 0.1 μM) to the mean CFP/YFP ratios before and after LH in wild-type follicles (see Fig. 3A), and used the "4PL" curve fitting function in Prism 6 (GraphPad Software, Inc., La Jolla, CA) to generate a four-parameter logistic model constrained to an EC_{50} of 0.5 μM and a Hill slope of 1 for cGi500 (Russwurm et al., 2007) (see Fig. 3E). This equation has the following form, where Y = CFP/YFP ratio, X = log(cGMP[μM]), A = upper CFP/YFP plateau, B = lower CFP/YFP plateau, C = log(EC_{50}[μM]), and D = Hill slope:

$$Y = B + \left(\frac{A - B}{1 + 10^{(C-X)D}}\right)$$

The model returned values of 2.39 and 1.24 for A and B, respectively, which we applied to the above equation (after rearranging to solve for X) and calculated cGMP concentrations ($\log_{10}$[μM]) from the individual plateau CFP/YFP ratios 20 min after LH in the three mutant genotypes. The means of these $\log_{10}$[μM] cGMP concentrations are plotted on the curve in Fig. 3E. The reported mean cGMP concentrations (μM) were calculated by antilog transformation of the individual estimated concentrations, followed by taking the mean for each genotype.

2.7. Nuclear envelope breakdown

To determine the time course of meiotic resumption, preovulatory follicles were treated with LH and oocytes were scored hourly for the presence of an intact nuclear envelope and nucleolus. Oocytes were considered to have undergone meiotic resumption when the nuclear envelope and nucleolus could no longer be seen. Oocytes were scored until either nuclear envelope breakdown (NEBD) occurred, or the oocyte could no longer be seen clearly due to cumulus expansion (Shuhaibar et al., 2016). For Fig. 4C and D, follicles were treated for one hour with the PDE5 inhibitor sildenafil (100 nM) prior to LH addition. After adding sildenafil or control vehicle (DMSO) to the medium in the dish, a droplet of the medium was placed on each follicle to ensure rapid exposure to the drug.

2.8. Statistical analysis

All analyses were conducted using Prism 6 (GraphPad Software, Inc., La Jolla, CA). Details are given in the figure legends.

3. Results and discussion

3.1. PDE5 is phosphorylated in response to LH in mouse ovarian follicles

Previously, we showed that LH signaling in rat ovarian follicles and rat granulosa cells causes serine 92 of PDE5 to be phosphorylated by PKA, and that this is correlated with an increase in PDE5 activity (Egbert et al., 2016). To establish a mouse model to test whether the phosphorylation of PDE5 caused the increase in its activity, we first investigated if LH signaling also phosphorylates PDE5 in mouse follicles. Lysates from follicles treated with LH or PBS for 30 min were separated on a gel containing Phos-tag, which retards the electrophoretic migration of phosphorylated proteins relative to non-phosphorylated proteins (Kinoshita et al., 2006; Egbert et al., 2014, 2016), and immunoblotted with a total PDE5 antibody. PDE5 from follicles without LH treatment migrated as a single band (Fig. 1B). However, LH treatment caused PDE5 to migrate as two bands, with one band

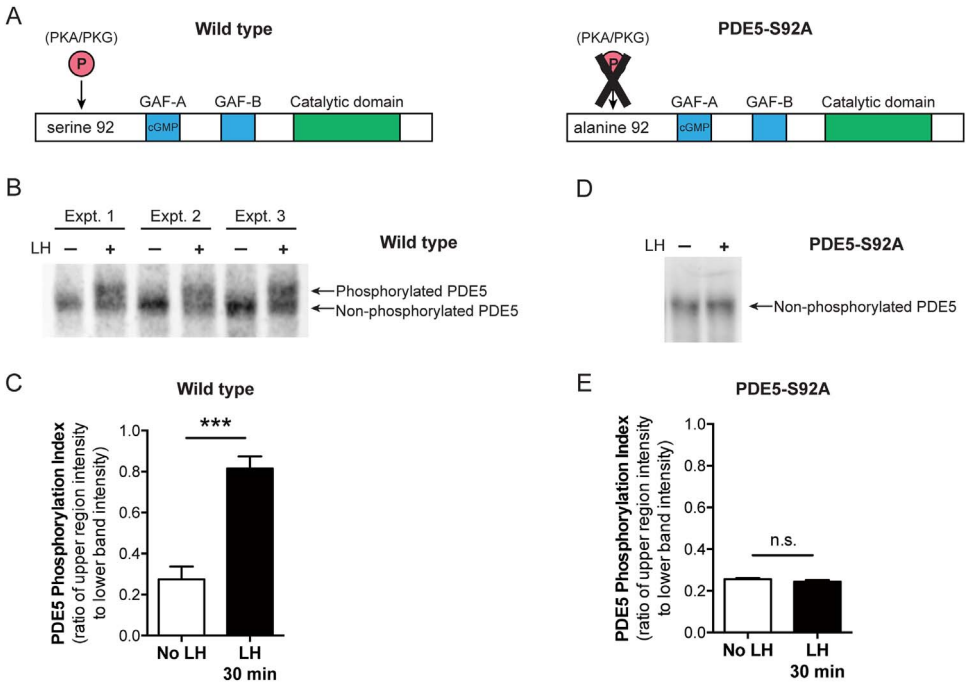

Fig. 1. LH signaling increases PDE5 phosphorylation on serine 92 in mouse ovarian follicles. (A) Left, diagram of wild-type PDE5 showing the sole PKA/PKG phosphorylation site on serine 92 near the cGMP-binding GAF-A domain. Right, diagram of PDE5 in which serine 92 was changed to alanine (PDE5-S92A), such that the protein cannot be phosphorylated. Modified from Egbert et al. (2016) and Bender and Beavo (2006) with permission. **(B)** Increase in PDE5 phosphorylation in wild-type follicles that were treated ± LH for 30 min. Lysates from follicles were run on a gel containing Phos-tag, which differentially slows the migration of phosphorylated proteins, and immunoblotted with a total PDE5 antibody. Upper and lower bands indicate phosphorylated and non-phosphorylated PDE5, respectively. Molecular weight standards are not shown because they do not correlate with protein size on a Phos-tag gel. **(C)** The PDE5 phosphorylation index, defined as the ratio of signal intensity between the region containing the phosphorylated (upper) PDE5 band and the region containing the non-phosphorylated (lower) band, increased with LH treatment in wild-type follicles. Mean ± SEM of 5 experiments, including those shown in **B**, is plotted. *** indicates $p < 0.001$ by unpaired *t*-test. **(D)** A single band was observed in follicles from $Pde5^{S92A/S92A}$ mice that were treated ± LH for 30 min, indicating that the mutation prevented PDE5 phosphorylation in response to LH. Lysates were processed as described for **B. (E)** The PDE5 phosphorylation index did not change with LH treatment in follicles from $Pde5^{S92A/S92A}$ mice. The index was measured as described for **C**. Mean ± SEM of 3 experiments, including the one shown in **D**; n.s. (not significant) indicates $p > 0.05$ by unpaired *t*-test.

migrating more slowly than the band seen in the control (Fig. 1B), indicating phosphorylation. To quantify this change, we calculated the ratio of the upper band intensity to the lower band intensity. This index of phosphorylation was significantly higher in follicles treated with LH (Fig. 1C). These data indicate that PDE5 becomes more phosphorylated in response to LH signaling in mouse follicles, as we previously reported for rat follicles and granulosa cells.

3.2. Generation of mice in which PDE5 cannot be phosphorylated

To test the functions of PDE5 phosphorylation in mouse follicles, we used CRISPR/Cas9 technology to generate a mouse with a global point mutation in *Pde5* that changes the sequence encoding serine 92 to encode alanine (*Pde5-S92A*), which cannot be phosphorylated (Fig. 1A, Supplementary Fig. S1). In follicles from mice homozygous for this mutation ($Pde5^{S92A/S92A}$), a single band was observed by Phos-tag regardless of LH treatment (Fig. 1D), and the index of phosphorylation was not different between groups (Fig. 1E). These data indicate that the mutation successfully blocked the LH-induced phosphorylation of serine 92, and also confirm that serine 92 is the only PDE5 site that is phosphorylated in response to LH.

3.3. LH signaling increases PDE5 hydrolytic activity by phosphorylation of serine 92

To test whether LH signaling increases PDE5 activity in mouse follicles, and whether such an increase is dependent on PDE5 phosphorylation, we measured the cGMP hydrolytic activity of PDE5 in follicles from wild-type and $Pde5^{S92A/S92A}$ mice. PDE5 activity was calculated as the difference between total cGMP-hydrolytic activity in the absence and presence of 30–100 nM sildenafil (Egbert et al., 2016). Although 30–100 nM sildenafil also inhibits PDE6 (Ballard et al., 1998; Corbin and Francis, 2002; Bischoff, 2004), western blotting did not detect proteins in mouse follicles that co-migrated with PDE6A and PDE6B from mouse retina, even though 200 times more follicle protein was used compared to retina (Fig. 2A,B). A third isoform, PDE6C, was not investigated because concentrations of PDE6C mRNA are much lower than that of PDE6A/B (Egbert et al., 2016; Supplementary Table 1). In contrast, PDE5 was clearly detected in mouse follicles with only 10–20 times more follicle protein compared to mouse lung (Fig. 2C). Therefore, we considered the sildenafil-sensitive activity to represent PDE5 activity (Fig. 2D).

In wild-type mouse follicles, LH treatment increased both total cGMP-hydrolytic activity (Supplementary Fig. S3A) and PDE5 activity (Fig. 2E, Supplementary Fig. S3B). PDE5 activity increased by an average of 26% compared to controls (Fig. 2E). However, in follicles from $Pde5^{S92A/S92A}$ mice, LH treatment did not increase either total cGMP-hydrolytic activity (Supplementary Fig. S3A) or PDE5 activity (Fig. 2E, Supplementary Fig. S3B), and in fact caused a marginally significant reduction in PDE5 activity, to an average of 15% below controls.

These measurements demonstrate that LH-induced phosphorylation of serine 92 is required for the increase in cGMP-hydrolytic activity of PDE5 in mouse follicles after LH treatment. The decrease in PDE5 activity following LH treatment in $Pde5^{S92A/S92A}$ follicles is not unexpected considering that cGMP binding to the GAF-A domain is the primary mechanism of PDE5 activation (Rybalkin et al., 2003; Bender and Beavo, 2006). Phosphorylation of PDE5 on serine 92 serves to further increase its hydrolytic activity by stabilizing the occupancy of cGMP at the GAF-A site (Corbin et al., 2000; Francis et al., 2002; Mullershausen et al., 2003; Rybalkin et al., 2003; Bender and Beavo, 2006; Jäger et al., 2010). In untreated follicles, resting cGMP levels are

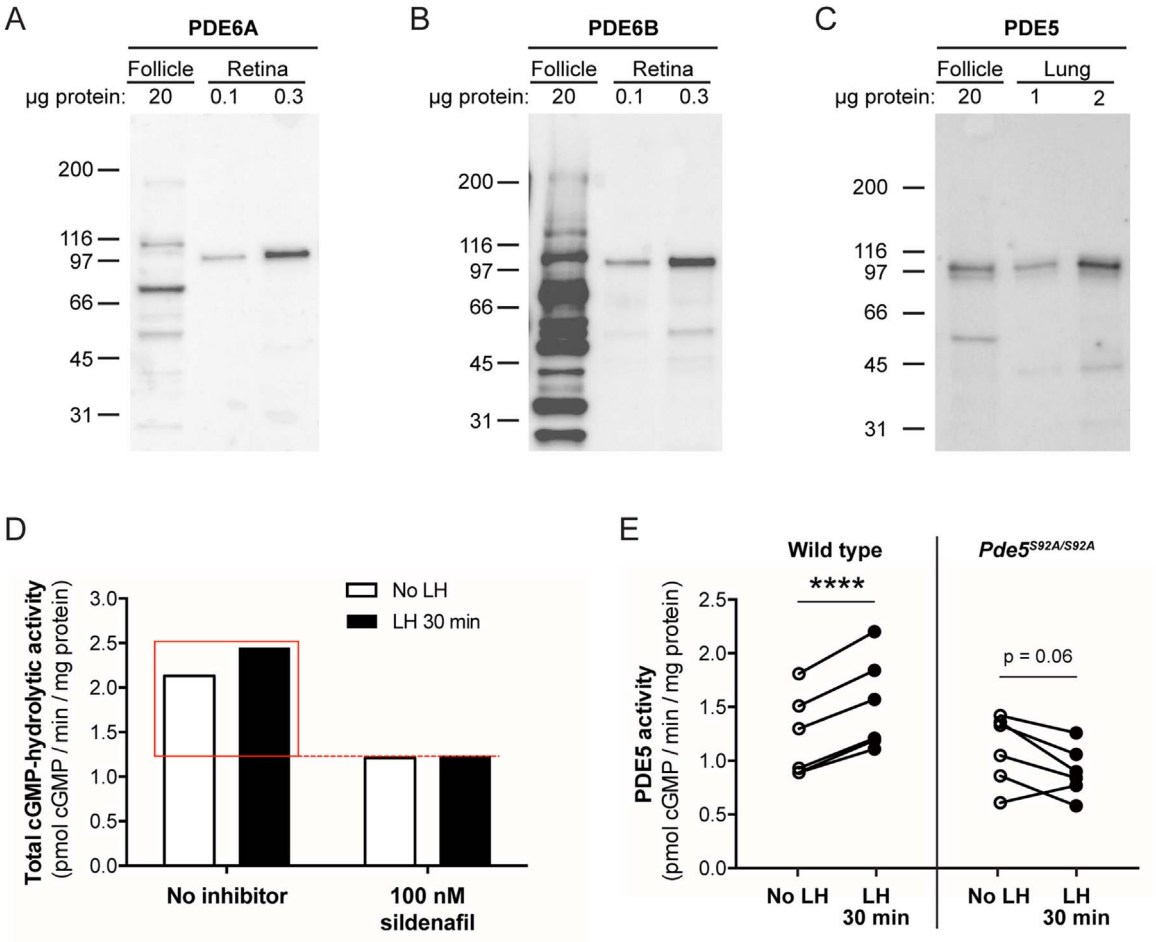

Fig. 2. Phosphorylation of PDE5 is required for the LH-induced increase in cGMP-hydrolytic activity of PDE5 in mouse follicles. (A-C) Western blots showing that follicles contain PDE5 but no detectable PDE6 protein, allowing sildenafil to be used as a specific inhibitor of PDE5 activity. **(A,B)** Western blot, following standard SDS-PAGE, showing PDE6A and PDE6B in mouse retina but not in mouse follicles, as indicated by the absence of a co-migrating band. The amount of follicle protein was up to 200 times that of retina. Molecular weight in kDa is shown at left. **(C)** Western blot showing that mouse follicles contain PDE5 at ~ 5–10% of the level in mouse lung. **(D)** Calculation of PDE5 activity from a representative assay. For each treatment, the sample was assayed for cGMP-hydrolytic activity in the absence and presence of 30–100 nM sildenafil. PDE5 activity was considered to be the sildenafil-sensitive activity outlined by the red box. **(E)** LH treatment increases PDE5 activity in wild-type follicles, but not in *Pde5*$^{S92A/S92A}$ follicles. For each experiment, follicles from either wild-type or *Pde5*$^{S92A/S92A}$ mice were split into two identical groups and treated with either control vehicle (PBS; open circles) or LH (filled circles) for 30 min. Lysates of these follicles were assayed for PDE5-specific cGMP hydrolytic activity; individual follicle pairs ± LH are connected by lines. In follicles from wild-type mice, the mean ± SEM increase in PDE5 activity after LH treatment was 26 ± 2%. However, in follicles from *Pde5*$^{S92A/S92A}$ mice, LH treatment did not increase PDE5 activity, and in fact, the mean ± SEM change indicated a marginally significant *decrease* of 15 ± 9%. Data were analyzed by paired *t*-test. **** indicates $p < 0.0001$.

high (~ 4 µM; Shuhaibar et al., 2015) such that PDE5 is partially activated by high GAF-A occupancy. After LH treatment, follicle cGMP levels fall, due in part to inactivation of the NPR2 guanylyl cyclase (Robinson et al., 2012; Egbert et al., 2014; Shuhaibar et al., 2016). In *Pde5*$^{S92A/S92A}$ follicles, where binding of cGMP to the GAF-A site cannot be stabilized by phosphorylation, falling cGMP levels would lead to less occupancy at the GAF-A site and thus explain the observed decrease in PDE5 activity.

The LH-induced increase in PDE5 activity in mouse follicles is somewhat smaller compared to what we previously reported in rat follicles (Egbert et al., 2016), and the reason for this difference is not clear. It is possible that phosphorylation of PDE5 is a more important mechanism for mediating the cGMP decrease in rat follicles, or that there are quantitative differences in either basal or LH-stimulated phosphorylation or cGMP occupancy at the regulatory GAF-A site that could account for the disparity between the two species. These would not be unexpected, as many differences have been observed between mouse and rat oocytes and follicles in their responses to various cyclic nucleotide mediators (Downs, 2011). Nevertheless, by using *Pde5*$^{S92A/S92A}$ mutant mice, we show that LH signaling increases PDE5 activity in ovarian follicles through phosphorylation.

3.4. PDE5 phosphorylation and activation contributes to the LH-induced cGMP decrease

Since the dephosphorylation and inactivation of NPR2 accounts for only part of the cGMP decrease after LH treatment of follicles (Egbert et al., 2014; Shuhaibar et al., 2016; compare the black and orange lines in Fig. 3C), we hypothesized that activation of one or more phosphodiesterases would account for the remainder of the decrease. We thus tested whether the LH-induced phosphorylation and increase in PDE5 activity contributes to the follicle cGMP decrease using mice that express the cGi500 FRET sensor for cGMP (Thunemann et al., 2013; Shuhaibar et al., 2015). cGi500 is composed one cyan fluorescent protein (CFP) and one yellow fluorescent protein (YFP) linked by two cGMP-binding domains (Russwurm et al., 2007). When CFP is excited by 436 nm light, energy can be transferred to YFP if they are in close proximity, leading to light emission from both proteins. Cyclic GMP binding to cGi500 changes its conformation such that CFP and YFP are farther apart, leading to less light emission from YFP as a result of CFP excitation. Thus, the ratio of CFP/YFP emission increases with cGMP binding to cGi500.

Follicles from both wild-type and *Pde5*$^{S92A/S92A}$ mice that also expressed cGi500 started with a similar baseline CFP/YFP ratio in the

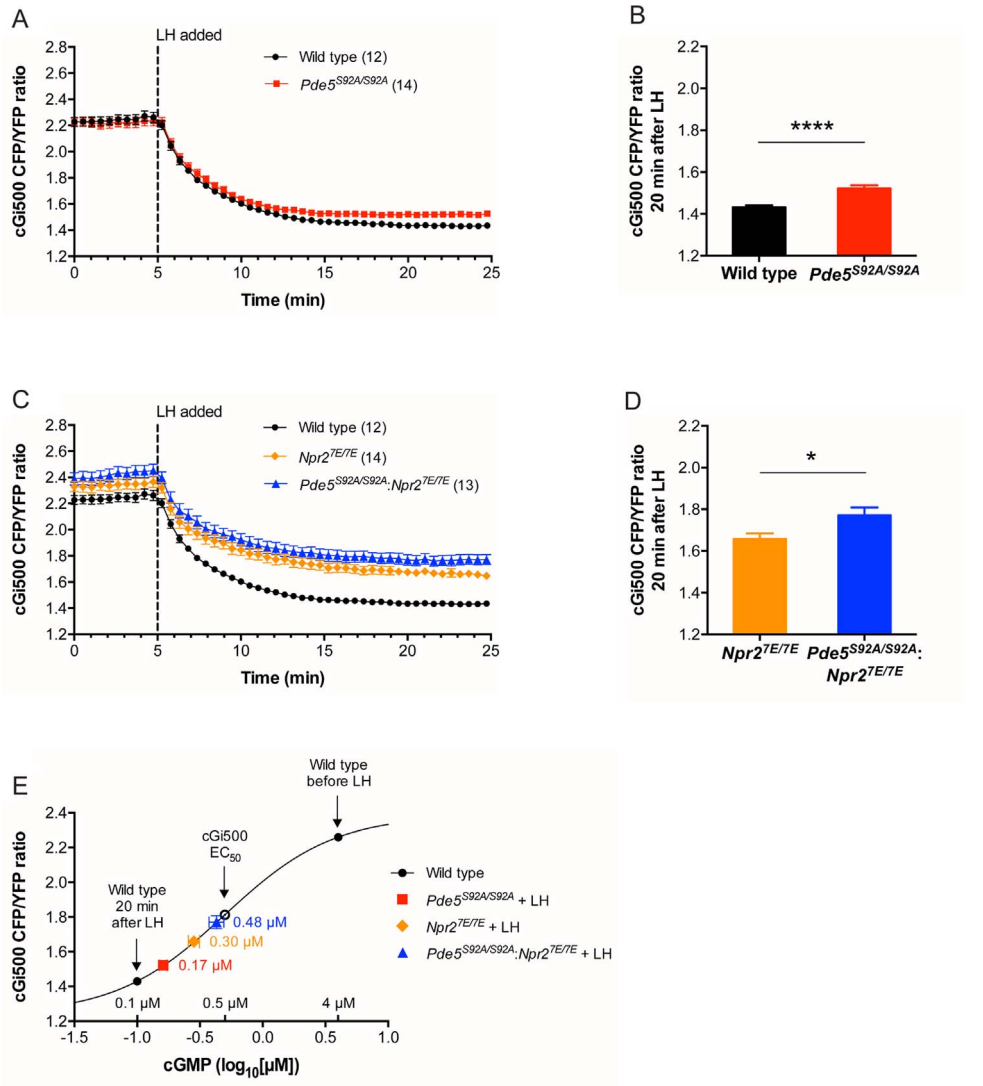

Fig. 3. Preventing the phosphorylation of PDE5 on serine 92 inhibits part of the LH-induced cGMP decrease. Follicles from wild-type, *Pde5*$^{S92A/S92A}$, *Npr2*$^{7E/7E}$, and *Pde5*$^{S92A/S92A}$:*Npr2*$^{7E/7E}$ mice that also express the cGi500 FRET sensor for cGMP were imaged every 30 s by confocal microscopy for 5 min before, and for 20 min after, the addition of LH. The ratio of CFP/YFP fluorescence is an indicator of cGMP concentration. Measurements were taken from the outer 25 µm of mural granulosa cells (see Shuhaibar et al., 2015). **(A)** Time course of the LH-induced cGMP decrease in follicles from wild-type (black) or *Pde5*$^{S92A/S92A}$ (red) mice. Each time point represents the mean ± SEM CFP/YFP ratio for the number of follicles shown in parentheses. **(B)** The mean CFP/YFP ratio 20 min after LH perfusion (average of the final 5 scans of the recordings shown in **A**) was significantly higher in *Pde5*$^{S92A/S92A}$ follicles compared to wild-type follicles (** indicates $p < 0.01$ by unpaired *t*-test). This indicates that the cGMP concentration after LH treatment is higher in follicles where PDE5 activity cannot be increased by phosphorylation. **(C)** Time course of the LH-induced cGMP decrease in follicles from *Npr2*$^{7E/7E}$ (orange) or *Pde5*$^{S92A/S92A}$:*Npr2*$^{7E/7E}$ (blue) mice. Each time point represents the mean ± SEM CFP/YFP ratio for the number of follicles shown in parentheses. For comparison, the wild-type data from **A** is also shown (black). **(D)** The mean CFP/YFP ratios 20 min after LH perfusion (average of the final 5 scans of the recordings shown in **C**) was significantly higher in *Pde5*$^{S92A/S92A}$:*Npr2*$^{7E/7E}$ follicles compared to *Npr2*$^{7E/7E}$ follicles (* indicates $p < 0.05$ by unpaired *t*-test). **(E)** Conversion of post-LH cGi500 CFP/YFP ratio values to approximate concentrations of cGMP in the follicles of mutant mice. Using an EC_{50} of 0.5 µM and a Hill Slope of 1 for cGi500, a four-parameter logistic model was fitted to the average CFP/YFP ratios in wild-type follicles before and 20 min after LH, which correspond to cGMP concentrations of ~ 4 µM and ~ 0.1 µM, respectively (see Section 2.6). Cyclic GMP concentrations (µM) for the reference points are shown on top of the x-axis. Follicle CFP/YFP ratios from mutant mice 20 min after LH (data shown in **B** and **D**) were used to calculate the approximate cGMP concentrations for each genotype. Symbols represent the mean ± SEM for both variables for the number of follicles given in **A** and **C**; where error bars are not visible, they are contained within the symbol.

mural granulosa layer, indicating no detectable difference in initial cGMP levels between genotypes (Fig. 3A). Based on ELISA measurements, the initial cGMP concentration is ~ 4 µM (Shuhaibar et al., 2015). After perfusion with LH, cGMP rapidly decreased in follicles of both genotypes, reaching a plateau CFP/YFP ratio at 20 min. In wildtype follicles, the plateau cGMP concentration is ~ 0.1 µM, as determined by ELISA (Shuhaibar et al., 2015). The plateau was slightly higher in *Pde5*$^{S92A/S92A}$ follicles, indicating that some of the cGMP decrease was prevented (Fig. 3A). Though the difference in plateau levels between the two genotypes was significant (Fig. 3B), it only accounted for ~ 10% of the total change in CFP/YFP ratio after LH.

We then considered the possibility that the small magnitude of the effect of the *Pde5-S92A* mutation on the LH-induced cGMP decrease could be due to a compensatory increase in the expression of another cGMP phosphodiesterase in these mutant mice. However, total cGMP-hydrolytic activity in the absence of LH was the same for *Pde5*$^{S92A/S92A}$ and wild-type follicles (Supplementary Fig. S3A). The sildenafil-sensitive (PDE5) and sildenafil-insensitive components of the total activity were also unaffected by the mutation (Supplementary Fig. S3B,C). These findings argued against a compensatory increase in another phosphodiesterase. Likewise, since the total cGMP-hydrolytic activity is unaffected by the *Pde5-S92A* mutation, the lack of effect of the mutation on the basal cGMP concentration (Fig. 3A) argues against a compensatory change in the expression of NPR2 or another guanylyl cyclase.

To test whether prevention of PDE5 phosphorylation has a greater effect on the LH-induced cGMP decrease when NPR2 cannot be

inactivated, we crossed the *Pde5-S92A* and *Npr2-7E* lines to generate mice homozygous for both mutations ($Pde5^{S92A/S92A}$:$Npr2^{7E/7E}$) and that also express cGi500. Follicles from these mice, as well as those for $Npr2^{7E/7E}$ mice, had higher baseline CFP/YFP ratios than wild-type follicles (Fig. 3C), presumably due to prevention of mechanisms that reduce cGMP levels. LH perfusion caused a similarly rapid decrease in the relative cGMP levels in $Npr2^{7E/7E}$ and $Pde5^{S92A/S92A}$:$Npr2^{7E/7E}$ follicles (Fig. 3C). The plateau CFP/YFP ratio 20 min after LH was significantly higher in follicles with both mutations (Fig. 3D).

In order to estimate cGMP concentrations from CFP/YFP ratios, we generated a calibration curve (Fig. 3E; see Section 2.6) based on ELISA measurements of cGMP in mouse follicles before LH (~ 4 μM) and after LH (~ 0.1 μM) reported by Shuhaibar et al. (2015). Note that these concentrations are based on an average follicle volume that is used as an estimate of the unknown total cytosolic volume (Norris et al., 2010). This analysis indicated that the plateau CFP/YFP ratios 20 min after LH in $Pde5^{S92A/S92A}$ follicles corresponded to a mean cGMP concentration of ~ 0.17 μM, compared to ~ 0.1 μM in wild-type follicles (Fig. 3E). The CFP/YFP ratio 20 min after LH in $Npr2^{7E/7E}$ follicles corresponded to a mean cGMP concentration of ~ 0.30 μM, and the ratio after LH treatment of follicles from $Pde5^{S92A/S92A}$:$Npr2^{7E/7E}$ mice corresponded to a mean cGMP concentration of ~ 0.48 μM (Fig. 3E). The *Pde5-S92A* mutation appears to prevent more of the cGMP decrease when combined with the *Npr2-7E* mutation, compared to the *Pde5-S92A* mutation alone. This suggests that there may be a synergistic interaction between the two mutations, but the functional importance is likely to be small. Furthermore, the cGMP concentrations are only estimates due to inexact information about cytosolic volume and other sources of experimental error in ELISA and FRET sensor measurements (see Norris et al., 2010; Shuhaibar et al., 2015). Since the cGMP concentration after LH treatment is at the lower end of the cGi500 dynamic range, future studies using a more sensitive cGMP FRET sensor (Götz et al., 2014; Calamera et al., 2017) could potentially provide more exact numbers. Regardless, our results indicate that an important component of the LH-induced decrease in follicle cGMP levels, from ~ 4 μM to ~ 0.5 μM, is not explained by NPR2 inactivation and PDE5 activation.

It remains to be investigated what other regulatory mechanisms account for the remainder of the cGMP decrease. A decrease in the activity of other membrane or soluble guanylyl cyclases is one possibility (see Sela-Abramovich et al., 2008), but this seems unlikely because follicles from mice with a loss-of-function mutation in *Npr2* have undetectable levels of cGMP (Geister et al., 2013), indicating that NPR2 is the dominant, and perhaps only, source of follicle cGMP. Thus, it is likely that at least one other phosphodiesterase is activated by LH signaling. PDE1 activity has been shown to contribute, along with PDE5, to the regulation of cGMP levels and oocyte meiotic resumption in rat follicles (Egbert et al., 2016). PDE1 is activated by calcium (Bender and Beavo, 2006); thus, if LH signaling elevates intracellular calcium within granulosa cells, PDE1 activity would increase and could provide a mechanism for at least part of the cGMP decrease. Though PDE1 and PDE5 together accounted for ~ 80% of basal, unstimulated cGMP-hydrolyzing activity in rat follicles (Egbert et al., 2016), other PDEs could also contribute to the LH-induced cGMP decrease.

3.5. Preventing PDE5 phosphorylation does not affect the timing of oocyte meiotic resumption

The primary function of the follicle cGMP decrease after LH

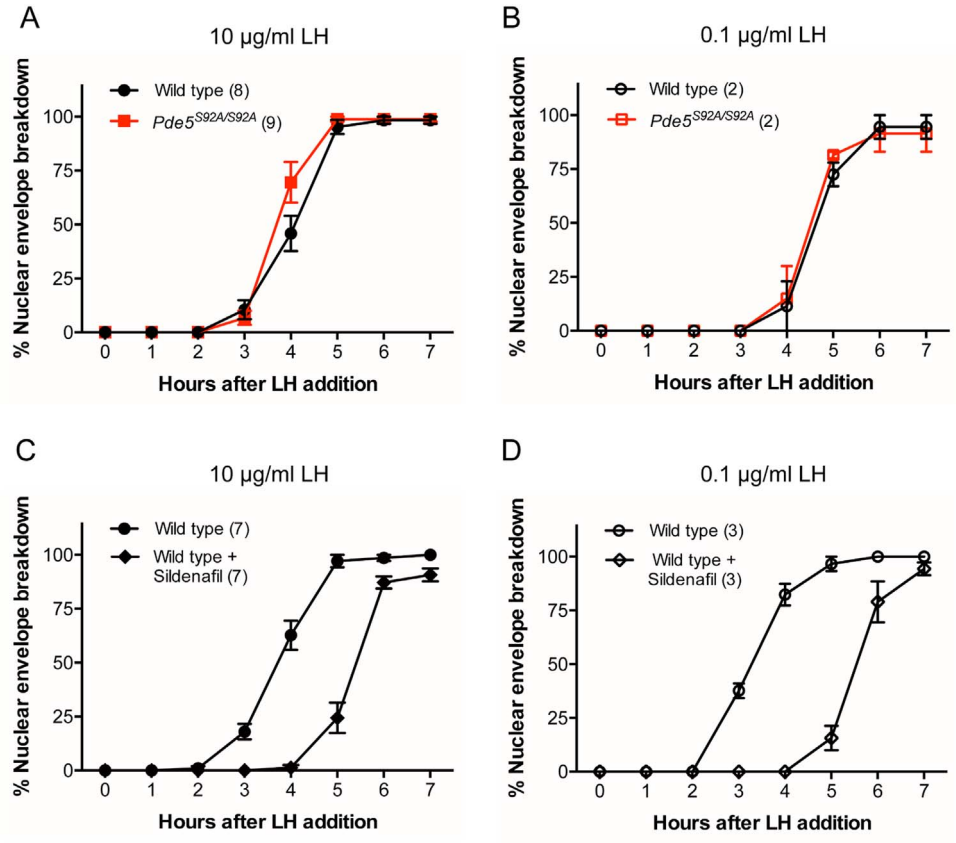

Fig. 4. PDE5 activity, but not the increase in PDE5 activity due to phosphorylation, is required for the normal time course of oocyte meiotic resumption in response to LH. (A, B) Follicle-enclosed oocytes from wild-type and $Pde5^{S92A/S92A}$ mice undergo nuclear envelope breakdown (NEBD) on a similar time scale in response to LH (**A**, 10 μg/ml LH; **B**, 0.1 μg/ml LH). Oocytes were visually scored for nuclear envelope breakdown before adding LH, and every hour thereafter. Graphs show the mean ± SEM for the number of experiments indicated in parentheses, each including 6–15 follicles. **(C,D)** Blocking PDE5 activity by pretreating wild-type follicles for one hour with 100 nM sildenafil delays LH-induced NEBD by 1.5–2 h (**C**, 10 μg/ml LH; **D**, 0.1 μg/ml LH). Graphs show the mean ± SEM for the number of experiments indicated in parentheses, each including 10–15 follicles.

exposure is to allow cGMP to diffuse out of the oocyte though gap junctions (Shuhaibar et al., 2015), which relieves the inhibition of meiotic progression (Jaffe and Egbert, 2017). To determine whether the phosphorylation of PDE5 affects the timing of oocyte meiotic resumption, we treated wild-type and *Pde5*$^{S92A/S92A}$ follicles with 10 μg/ml LH and checked hourly for the presence of a nuclear envelope and nucleolus; disappearance of these structures indicates meiotic resumption (Norris et al., 2007). Follicles from both genotypes underwent NEBD on an identical time scale (Fig. 4A), indicating that the modest inhibition of the cGMP decrease observed in the mural granulosa cells of *Pde5*$^{S92A/S92A}$ follicles has no effect on the kinetics of meiotic resumption. To test whether the *Pde5-S92A* mutation may have a larger effect when follicles are stimulated with a less than saturating concentration of LH, we assessed the rate of NEBD in wild-type and *Pde5*$^{S92A/S92A}$ follicles in response to 0.1 μg/ml LH and found no difference between the two genotypes (Fig. 4B). Correspondingly, the *Pde5-S92A* mutation caused no obvious defect in fertility (Supplementary Fig. S2).

In contrast, pre-incubation of wild-type follicles for one hour with a selective inhibitor of PDE5 activity (100 nM sildenafil) delayed oocyte meiotic resumption in response to LH; the time to 50% NEBD was ~ 1.5–2 h longer in the presence of sildenafil (Fig. 4C and D). Similar results were obtained when using 10 μg/ml LH (Fig. 4C) or 0.1 μg/ml LH (Fig. 4D). These data are in agreement with previous studies in mouse (Vaccari et al., 2009) and rat (Egbert et al., 2016) indicating that PDE5 is a constitutive regulator of cGMP in follicles and is an important mediator of the cGMP decrease that leads to meiotic resumption. Thus, while PDE5 activity is required for the normal time course of meiotic resumption in mice, the *increase* in activity due to PDE5 phosphorylation is not required. The timing of meiotic resumption in response to LH in follicles isolated from *Pde5*$^{S92A/S92A}$:*Npr2*$^{7E/7E}$ double mutant mice was not assessed because the *Npr2-7E* mutation alone delays NEBD by ~ 5 h (Shuhaibar et al., 2016). At this time, cumulus expansion severs the connection between the granulosa cells and the oocyte (Eppig, 1982), thus disconnecting the supply of inhibitory cGMP to the oocyte, such that cGMP in the oocyte decreases and meiosis proceeds (Norris et al., 2008, 2009).

4. Conclusions

In mouse preovulatory follicles, LH signaling stimulates phosphorylation of PDE5, which increases its cGMP-hydrolyzing activity by ~ 25%. To test the functional significance of this regulation, we generated mice with a point mutation that prevents PDE5 phosphorylation by changing serine 92 to alanine (*Pde5*$^{S92A/S92A}$). Using follicles from these mice, we showed that the increase in PDE5 activity due to phosphorylation contributes a relatively small component to the total cGMP decrease in mural granulosa cells in response to LH. Furthermore, preventing PDE5 phosphorylation had no effect on the timing of meiotic resumption, which is dependent on a decrease in cGMP levels in the follicle and oocyte. Thus, the function of rapid PDE5 phosphorylation in lowering cGMP in mouse follicles appears to be redundant. Though the effect of PDE5 phosphorylation on cGMP levels appears to be small in mouse follicles, *Pde5*$^{S92A/S92A}$ mutant mice could be useful to study the regulation of cGMP levels in other cell and developmental processes such as axon bifurcation (Ter-Avetisyan et al., 2014), bone elongation (Nakao et al., 2015), cardiomyocyte proliferation (Becker et al., 2014), and the regulation of smooth muscle contraction (Rybalkin et al., 2002).

We estimated the post-LH concentration of cGMP in *Pde5*$^{S92A/S92A}$ follicles, which undergo NEBD with a time course identical to wild type, to be ~ 0.17 μM, compared to an estimated post-LH cGMP concentration of ~ 0.30 μM in *Npr2*$^{7E/7E}$ follicles, in which NEBD is inhibited (Shuhaibar et al., 2016). Thus, cGMP concentrations must fall dramatically for meiotic resumption to occur normally. The threshold concentration of cGMP for triggering meiotic resumption is estimated to lie between ~ 0.30 μM and ~ 0.17 μM, compared to the initial 4 μM level before LH exposure. As mentioned above, several factors limit the precision of these numbers, but nevertheless, they indicate that the threshold is only slightly higher than the cGMP concentration attained normally in response to LH (~ 0.1 μM).

Since much of the LH-induced cGMP decrease remains unexplained after accounting for NPR2 inactivation and the increase in PDE5 activity, it is likely that LH signaling activates one or more additional phosphodiesterases to account for the rest of the cGMP decrease. A primary candidate is PDE1, which is expressed in mouse follicles (Conti et al., 1984) and is responsible for a substantial amount of basal cGMP-hydrolytic activity in rat follicles (Egbert et al., 2016). PDE1 is activated by calcium, and an increase in cytosolic calcium was seen when LH was applied to granulosa cells isolated from immature porcine ovaries (Flores et al., 1998). However, it is unknown if LH signaling causes calcium to increase in the granulosa cells of intact preovulatory follicles. With the availability of mouse lines that express fluorescent sensors for calcium (Madisen et al., 2015), it will be possible to investigate whether LH signaling increases calcium in the follicle, and thus stimulates cGMP hydrolysis by PDE1.

Acknowledgements

We thank Robert Feil for providing the cGi500 mice, Joseph Beavo, Kimberly Dodge-Kafka, Matthew Movsesian, Michael Russwurm, Sergei Rybalkin, and Mark Terasaki for helpful discussions, and Deborah Kaback, Katie Lowther, Kristine Mack, Leia Shuhaibar, Ninna Shuhaibar, Tracy Uliasz, and Giulia Vigone for advice and assistance with experiments. This work was supported by the Eunice Kennedy Shriver National Institute of Child Health and Human Development (R37HD014939 to LAJ).

Conflicts of interest

None.

Appendix A. Supporting information

Supplementary data associated with this article can be found in the online version at doi:10.1016/j.ydbio.2018.01.008.

References

Ballard, S.A., Gingell, C.J., Tang, K., Turner, L.A., Price, M.E., Naylor, A.M., 1998. Effects of sildenafil on the relaxation of human corpus cavernosum tissue in vitro and on the activities of cyclic nucleotide phosphodiesterase isozymes. J. Urol. 159, 2164–2171. http://dx.doi.org/10.1016/S0022-5347(01)63299-3.

Becker, J.R., Chatterjee, S., Robinson, T.Y., Bennett, J.S., Panáková, D., Galindo, C.L., Zhong, L., Shin, J.T., Coy, S.M., Kelly, A.E., Roden, D.M., Lim, C.C., MacRae, C.A., 2014. Differential activation of natriuretic peptide receptors modulates cardiomyocyte proliferation during development. Development 141. http://dx.doi.org/10.1242/dev.100370.

Bender, A.T., Beavo, J.A., 2006. Cyclic nucleotide phosphodiesterases: molecular regulation to clinical use. Pharmacol. Rev. 58, 488–520. http://dx.doi.org/10.1124/pr.58.3.5.

Bischoff, E., 2004. Potency, selectivity, and consequences of nonselectivity of PDE inhibition. Int J. Impot. Res. 16, S11–S14. http://dx.doi.org/10.1038/sj.ijir.3901209.

Calamera, G., Bjørnerem, M., Ulsund, A.H., Kim, J.J., Kim, C., Levy, F.O., Andressen, K.W., 2017. Development of FRET-based sensors with nanomolar affinity for cGMP using structure-based design. BMC Pharmacol. Toxicol. 18 (Suppl 1), A36. http://dx.doi.org/10.1186/s40360-017-0170-5.

Conti, M., Kasson, B.G., Hsueh, A.J.W., 1984. Hormonal regulation of 3′,5′-adenosine monophosphate phosphodiesterases in cultured rat granulosa cells. Endocrinology 114, 2361–2368. http://dx.doi.org/10.1210/endo-114-6-2361.

Corbin, J.D., Francis, S.H., 2002. Pharmacology of phosphodiesterase-5 inhibitors. Int. J. Clin. Pract. 56, 453–459, (PMID:12166544).

Corbin, J.D., Turko, I.V., Beasley, A., Francis, S.H., 2000. Phosphorylation of phosphodiesterase-5 by cyclic nucleotide-dependent protein kinase alters its catalytic and allosteric cGMP-binding activities. Eur. J. Biochem. 267, 2760–2767. http://dx.doi.org/10.1046/j.1432-1327.2000.01297.x.

Davies, S.P., Reddy, H., Caivano, M., Cohen, P., 2000. Specificity and mechanism of

action of some commonly used protein kinase inhibitors. Biochem. J. 351, 95–105 https://doi.org/10.1042/bj3510095.

Downs, S.M., 2011. Mouse versus rat: profound differences in meiotic regulation at the level of the isolated oocyte. Mol. Reprod. Dev. 78, 778–794. http://dx.doi.org/10.1002/mrd.21377.

Egbert, J.R., Shuhaibar, L.C., Edmund, A.B., Van Helden, D.A., Robinson, J.W., Uliasz, T.F., Baena, V., Geerts, A., Wunder, F., Potter, L.R., Jaffe, L.A., 2014. Dephosphorylation and inactivation of the NPR2 guanylyl cyclase in the granulosa cells contributes to the LH-induced cGMP decrease that causes resumption of meiosis in rat oocytes. Development 141, 3594–3604. http://dx.doi.org/10.1242/dev.112219.

Egbert, J.R., Uliasz, T.F., Shuhaibar, L.C., Geerts, A., Wunder, F., Kleiman, R.J., Humphrey, J.M., Lampe, P.D., Artemyev, N.O., Rybalkin, S.D., Beavo, J.A., Movsesian, M.A., Jaffe, L.A., 2016. Luteinizing hormone causes phosphorylation and activation of the cyclic GMP phosphodiesterase PDE5 in rat ovarian follicles, contributing, together with PDE1 activity, to the resumption of meiosis. Biol. Reprod. 94, 110. http://dx.doi.org/10.1095/biolreprod.115.135897.

Eppig, J.J., 1982. The relationship between cumulus cell-oocyte coupling, oocyte meiotic maturation, and cumulus expansion. Dev. Biol. 89, 268–272. http://dx.doi.org/10.1016/0012-1606(82)90314-1.

Flores, J.A., Aguirre, C., Sharma, O.P., Veldhuis, J.D., 1998. Luteinizing hormone (LH) stimulates both intracellular calcium ion ($[Ca^{2+}]_i$) mobilization and transmembrane cation influx in single ovarian (granulosa) cells: recruitment as a cellular mechanism of LH-$[Ca^{2+}]_i$ dose response. Endocrinology 139, 3606–3612. http://dx.doi.org/10.1210/endo.139.8.6162.

Francis, S.H., Bessay, E.P., Kotera, J., Grimes, K.A., Liu, L., Thompson, W.J., Corbin, J.D., 2002. Phosphorylation of isolated human phosphodiesterase-5 regulatory domain induces an apparent conformational change and increases cGMP binding affinity. J. Biol. Chem. 277, 47581–47587. http://dx.doi.org/10.1074/jbc.M206088200.

Geister, K.A., Brinkmeier, M.L., Hsieh, M., Faust, S.M., Karolyi, I.J., Perosky, Kozloff, J.E., Conti, K.M., Camper, M., 2013. SA. A novel loss-of-function mutation in Npr2 clarifies primary role in female reproduction and reveals a potential therapy for acromesomelic dysplasia, Maroteaux type. Hum. Mol. Genet. 22, 345–357. http://dx.doi.org/10.1093/hmg/dds432.

Götz, K.R., Sprenger, J.U., Perera, R.K., Steinbrecher, J.H., Lehnart, S.E., Kuhn, M., Gorelik, J., Balligand, J.-L., Nikolaev, V.O., 2014. Transgenic mice for real-time visualization of cGMP in intact adult cardiomyocytes. Circ. Res. 114, 1235–1245. http://dx.doi.org/10.1161/CIRCRESAHA.114.302437.

Hunzicker-Dunn, M., Mayo, K., 2014. Gonadotropin signaling in the ovary. In: Plant, T.M., Zeleznik, A.J. (Eds.), Knobil and Neill's Physiology of Reproduction4th ed.. Academic Press, San Diego, 895–945. http://dx.doi.org/10.1016/B978-0-12-397175-3.00020-X.

Jaffe, L.A., Egbert, J.R., 2017. Regulation of mammalian oocyte meiosis by intercellular communication within the ovarian follicle. Ann. Rev. Physiol. 79, 237–260. http://dx.doi.org/10.1146/annurev-physiol-022516-034102.

Jäger, R., Schwede, F., Genieser, H.-G., Koesling, D., Russwurm, M., 2010. Activation of PDE2 and PDE5 by specific GAF ligands: delayed activation of PDE5. Br. J. Phamacol. 161, 1645–1660. http://dx.doi.org/10.1111/j.1476-5381.2010.00977.x.

Kinoshita, E., Kinoshita-Kikuta, E., Takiyama, K., Koike, T., 2006. Phosphate-binding tag, a new tool to visualize phosphorylated proteins. Mol. Cell. Proteom. 5, 749–757. http://dx.doi.org/10.1074/mcp.T500024-MCP200.

Madisen, L., Garner, A.R., Shimaoka, D., Chuong, A.S., Klapoetke, N.C., Li, L., van der Bourg, A., Niino, Y., Monetti, C., Gu, H., Mills, M., Cheng, A., Tasic, B., Nguyen, T.N., Sunkin, S.M., Benucci, A., Nagy, A., Miyawaki, A., Helmchen, F., Empson, R.M., Knöpfel, T., Boyden, E.S., Reid, R.C., Carandini, M., Zeng, H., 2015. Transgenic mice for intersectional targeting of neural sensors and effectors with high specificity and performance. Neuron 85, 942–958. http://dx.doi.org/10.1016/j.neuron.2015.02.022.

Mehlmann, L.M., Kalinowski, R.R., Ross, L.F., Parlow, A.F., Hewlett, E.L., Jaffe, L.A., 2006. Meiotic resumption in response to luteinizing hormone is independent of a Gi family G protein or calcium in the mouse oocyte. Dev. Biol. 299, 345–355. http://dx.doi.org/10.1016/j.ydbio.2006.07.039.

Mullershausen, F., Friebe, A., Feil, R., Thompson, W.J., Hofman, F., Koesling, D., 2003. Direct activation of PDE5 by cGMP: long-term effects within NO/cGMP signaling. J. Cell Biol. 160, 719–727. http://dx.doi.org/10.1083/jcb.200211041.

Murray, A.J., 2008. Pharmacological PKA inhibition: all may not be what it seems. Sci. Signal. 1 (22), re4. http://dx.doi.org/10.1126/scisignal.122re4.

Nakao, K., Osawa, K., Yasoda, A., Yamanaka, S., Fujii, T., Kondo, E., Koyama, N., Kanamoto, N., Miura, M., Kuwahara, K., Akiyama, H., Bessho, K., Nakao, K., 2015. The local CNP/GC-B system in growth plate is responsible for endochondral bone growth. Sci. Rep. 5, 10554. http://dx.doi.org/10.1038/srep10554.

Norris, R.P., Freudzon, L., Freudzon, M., Hand, A.R., Mehlmann, L.M., Jaffe, L.A., 2007. A Gs-linked receptor maintains meiotic arrest in mouse oocytes, but luteinizing hormone does not cause meiotic resumption by terminating receptor-Gs signaling. Dev. Biol. 310, 240–249. http://dx.doi.org/10.1016/j.ydbio.2007.07.017.

Norris, R.P., Freudzon, M., Mehlmann, L.M., Cowan, A.E., Simon, A.M., Paul, D.L., Lampe, P.D., Jaffe, L.A., 2008. Luteinizing hormone causes MAP kinase-dependent phosphorylation and closure of connexin 43 gap junctions in mouse ovarian follicles: one of two pathways to meiotic resumption. Development 135, 3229–3238. http://dx.doi.org/10.1242/dev.025494.

Norris, R.P., Ratzan, W.J., Freudzon, M., Mehlmann, L.M., Krall, J., Movsesian, M.A., Wang, H., Ke, H., Nikolaev, V.O., Jaffe, L.A., 2009. Cyclic GMP from the surrounding somatic cells regulates cyclic AMP and meiosis in the mouse oocyte. Development 136, 1869–1878. http://dx.doi.org/10.1242/dev.035238.

Norris, R.P., Freudzon, M., Nikolaev, V.O., Jaffe, L.A., 2010. Epidermal growth factor receptor kinase activity is required for gap junction closure and for part of the decrease in ovarian follicle cGMP in response to LH. Reproduction 140, 655–662. http://dx.doi.org/10.1530/REP-10-0288.

Potter, L.R., 2011. Regulation and therapeutic targeting of peptide-activated receptor guanylyl cyclases. Pharmacol. Ther. 130, 71–82. http://dx.doi.org/10.1016/j.pharmthera.2010.12.005.

Richard, S., Baltz, J.M., 2017. Preovulatory suppression of mouse oocyte cell volume-regulatory mechanisms is via signalling that is distinct from meiotic arrest. Sci. Rep. 7, 702. http://dx.doi.org/10.1038/s41598-017-00771-y.

Robinson, J.W., Zhang, M., Shuhaibar, L.C., Norris, R.P., Geerts, A., Wunder, F., Eppig, J.J., Potter, L.R., Jaffe, L.A., 2012. Luteinizing hormone reduces the activity of the NPR2 guanylyl cyclase in mouse ovarian follicles, contributing to the cyclic GMP decrease that promotes resumption of meiosis in oocytes. Dev. Biol. 366, 308–316. http://dx.doi.org/10.1016/j.ydbio.2012.04.019.

Russwurm, M., Mullershausen, F., Friebe, A., Jäger, R., Russwurm, C., Koesling, D., 2007. Design of fluorescent resononance energy transfer (FRET)-based cGMP indicators: a systematic approach. Biochem. J. 407, 69–77. http://dx.doi.org/10.1042/BJ20070348.

Rybalkin, S.D., Rybalkina, I.G., Feil, R., Hofmann, F., Beavo, J.A., 2002. Regulation of cGMP-specific phosphodiesterase (PDE5) phosphorylation in smooth muscle cells. J. Biol. Chem. 277, 3310–3317. http://dx.doi.org/10.1074/jbc.M106562200.

Rybalkin, S.D., Rybalkina, I.G., Shimizu-Albergine, M., Tang, X.-B., Beavo, J.A., 2003. PDE5 is converted to an activated state upon cGMP binding to the GAF A domain. EMBO J. 23, 469–478. http://dx.doi.org/10.1093/emboj/cdg051.

Sela-Abramovich, S., Galiani, D., Nevo, N., Dekel, N., 2008. Inhibition of rat oocyte maturation and ovulation by nitric oxide: mechanism of action. Biol. Reprod. 78, 1111–1118. http://dx.doi.org/10.1095/biolreprod.107.065490.

Shuhaibar, L.C., Egbert, J.R., Norris, R.P., Lampe, P.D., Nikolaev, V.O., Thunemann, M., Wen, L., Feil, R., Jaffe, L.A., 2015. Intercellular signaling via cyclic GMP diffusion through gap junctions in the mouse ovarian follicle. Proc. Natl. Acad. Sci. USA 112, 5527–5532. http://dx.doi.org/10.1073/pnas.1423598112.

Shuhaibar, L.C., Egbert, J.R., Edmund, A.B., Uliasz, T.F., Dickey, D.M., Yee, S.-P., Potter, L.R., Jaffe, L.A., 2016. Dephosphorylation of juxtamembrane serines and threonines of the NPR2 guanylyl cyclase is required for rapid resumption of oocyte meiosis in response to luteinizing hormone. Dev. Biol. 409, 194–201. http://dx.doi.org/10.1016/j.ydbio.2015.10.025.

Stocco, C., Telleria, C., Gibori, G., 2007. The molecular control of corpus luteum formation, function, and regression. Endocr. Rev. 28, 117–149. http://dx.doi.org/10.1210/er.2006-0022.

Ter-Avetisyan, G., Rathjen, F.G., Schmidt, H., 2014. Bifurcation of axons from cranial sensory neurons is disabled in the absence of Npr2-induced cGMP signaling. J. Neurosci. 34, 737–747. http://dx.doi.org/10.1523/JNEUROSCI.4183-13.2014.

Thunemann, M., Wen, L., Hillenbrand, M., Vachaviolos, A., Feil, S., Ott, T., Han, X., Fukumura, D., Jain, R.K., Russwurm, M., de Wit, C., Feil, R., 2013. Transgenic mice for cGMP imaging. Circ. Res 113, 365–371. http://dx.doi.org/10.1161/CIRCRESAHA.113.301063.

Vaccari, S., Weeks, J.L., Hsieh, M., Menniti, F.S., Conti, M., 2009. Cyclic GMP signaling is involved in the LH-dependent meiotic maturation of mouse oocytes. Biol. Reprod. 81, 595–604. http://dx.doi.org/10.1095/biolreprod.109.077768.

Yoder, A.R., Robinson, J.W., Dickey, D.M., Andersland, J., Rose, B.A., Stone, M.D., Griffin, T.J., Potter, L.R., 2012. A functional screen provides evidence for a conserved, regulatory, juxtamembrane phosphorylation site in guanylyl cyclase A and B. PLoS One 7, e36747. http://dx.doi.org/10.1371/journal.pone.0036747.

Zhang, M., Su, Y.Q., Sugira, K., Xia, G., Eppig, J.J., 2010. Granulosa cell ligand NPPC and its receptor NPR2 maintain meiotic arrest in mouse oocytes. Science 330, 366–369. http://dx.doi.org/10.1126/science.1193573.